Electronic Supplementary Material (ESI) for RSC Advances.

Supplementary Information: Molecular structure characterization of asphaltene in the presence of inhibitors with nanoemulsions

Mahmoud Alhreez [a], and Dongsheng Wen [b, a]

[a] School of Chemical and Process Engineering, University of Leeds, Leeds, UK.

[b] School of Aeronautic Science and Engineering, Beihang University, Beijing, China.

Email address: d.wen@leeds.ac.uk

S1. Synthesis of nanoemulsions with the presence of AI

In the beginning, one sample containing DBSA and xylene was mixed together by stirring using a magnetic stirrer at 1000 rpm at room temperature for 24 hours until a clear sample was obtained. Simultaneously, another sample consisting of Tween 80, SDS, and deionized water were mixed together and added slowly to the mixture of xylene and DBSA. Then, the sample was sonicated by an ultrasonic probe for 8 minutes per sample. The procedure of synthesis of NEs with the presence and absence of AI was reported in the previous study [1], as depicted in the schematic diagram in **Figure S1**.

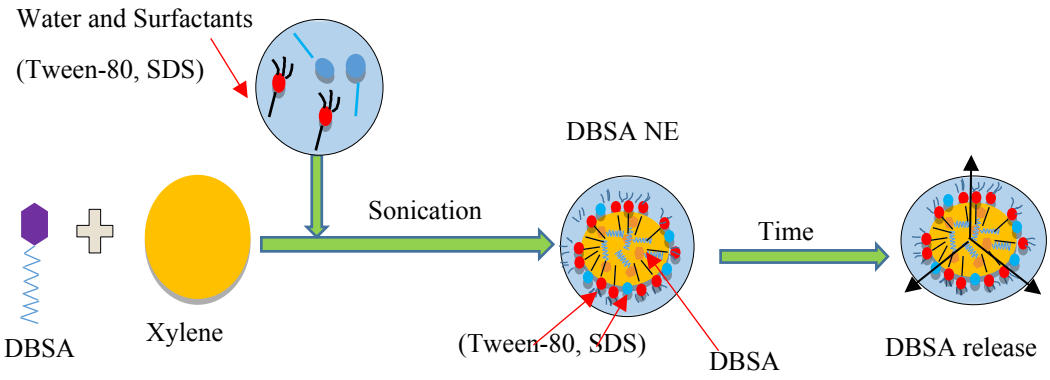

Figure S1: Schematic diagram of the synthesis procedure of DBSA NE and the release kinetics during a long time.

S2. XRD analysis

One of the best descriptions of the asphaltene structure was proposed by Yen 1974 [2]. He suggested molecular weights of 1- 5×10^3 Da, a molecular formula of nearly $(C_{79}H_{92}N_2S_2O)_3$, and molecular shape as shown in **Figure S2**. The whole asphaltene structure is containing from 8 to 16 fused rings might be placed at distances of 0.30 - 0.37 nm and linked by different systems such as ether, sulphide, aliphatic chain and/or naphthene ring linkages. The condensed sheets may also contain heteroatoms such as oxygen, sulfur, and nitrogen atoms which could act as free radicals for anchor points of bound metals such as Ni, V, Mo or Fe. The asphaltene cluster would be 0.8 – 1.6 nm in diameter and 1.6 – 2 nm in height.

XRD is utilized to study the molecular structure and the crystallite parameters of the asphaltene clusters **[3].** The procedure for calculating the crystalline parameters are presented below:

- The distance between two aromatic sheets d_m, were calculated using the Bragg equation:

$$d_m = \frac{\lambda}{\sin\theta 002} \quad \text{..... Eq. (S1)}$$

- The distance between the two aliphatic chains or interchain layer distance $d\gamma$ was calculated by using an equation:

$$d\gamma = \frac{5\,\lambda}{8\sin\theta\gamma} \quad \text{..... Eq. (S2)}$$

- The cluster diameter L_c was calculated by using the following equation:

$$L_c = \frac{0.45}{FWHM}$$ ..... Eq. (S3)

Where λ = 1.54055 Å; θ_γ and θ_{002} are the diffraction angles of γ and *002* bands, respectively; *FWHM* is the full width at half maximum, obtained from XRD analyses by using Origin 2017 software as shown in **Table S1**.

- The average number of aromatic sheets M_e were also calculated from Eqs. (S1) and (S3) as:

$$M_e = \frac{L_C}{d_m} + 1$$ ..... Eq. (S4)

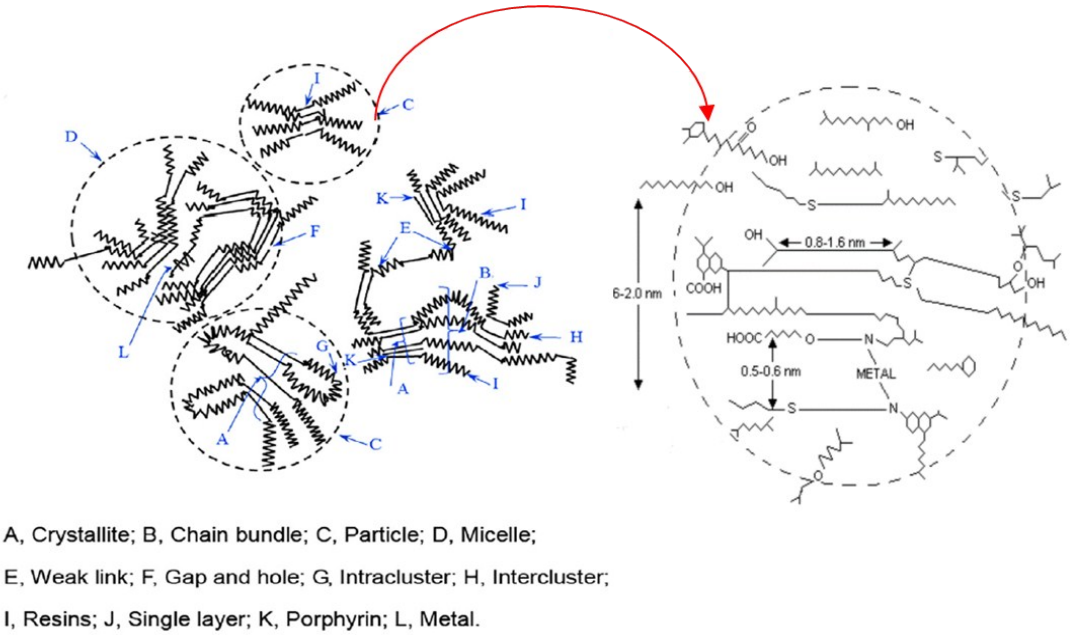

Figure S2: The molecular structure of asphaltene, Zig-zag lines represent saturated sheets or naphthenic rings; the straight lines represent the edge of flat sheets of condensed aromatic rings.

Table S1: XRD values obtained from Origin 2017 software.

	Asphaltene	With DBSA	With blank NE	With DBSA NE
$2\theta\gamma$	19.68	20.1	20.92	20.85
$2\theta_{002}$	26.5	22.9	24.0	22.2
$FWHM_{002\,-\,band}$	0.012	0.043	0.039	0.044
$FWHM_{10\,-\,band}$	0.129	0.148	0.137	0.15

S2. Characteristic peaks of FTIR bands of asphaltene

FTIR spectroscopy analysis confirmed that the asphaltene molecules contained primarily of linear, branched, and naphthenic hydrocarbons linked to large aromatic clusters [1,4,7]. More than 90% of hydrogen was found substituted on aliphatic groups [4]. Especially, -OH absorption bands were divided into six types on FTIR spectra as shown in **Table S2**.

Table S2: Functional groups present in asphaltenes by infrared spectroscopy.

Functional Group	**Absorption Band (cm^{-1})**	**Ref.**
- OH, - NH stretch	3600–3300	[4,5]
OH-π hydrogen bond	3530	[5]
Self-associated *n*-mers (n >3)	3400	[6]
OH- ether O hydrogen bonds	3280	[7]
Tightly bound cyclic OH tetramers	3150	[6]
OH- N (/base structures)	2940	[6]

COOH dimmers	2640	[6]
Aromatic hydrogen	3050	[4]
Aliphatic hydrogen	2993, 2920	[5]
- CH, - CH_2, - CH_3 stretching regions	3000–2800	[4]
-SH stretching regions	~2500	[8]
C = O	1800–1600	[6]
Keton (C = O stretching)	1735–1705	[5]
Aldehide (C = O stretching)	1740–1730	[4]
Conjugated C = C	1650, 1600	[4]
Aromatic C = C	1602	[7]
-CH, -CH_2, -CH_3 bending regions	1450–1375	[5]
Methyl bending vibrations	1377	[6]
Ether or ester group	1306	[5]
Ester linkage	1032	[9]
Sulfoxide groups	1030	[9]
C - S, C - O, C - N stretching regions	~1000	[4]
Aromatic C- H bending	900–700	[4]
Alkyl chain longer than four methylene groups	725–720	[5]

References

[1] Alhreez, M. and Wen, D., Controlled releases of asphaltene inhibitors by nanoemulsions, *Fuel, 2018*, *234*, 538-548.

[2] Yen, T.F., Structure of petroleum asphaltene and its significance, *Energy Sources, Part Arecovery, Utilization, And Environmental Effects*, 1974, 1(4), 447-463.

[3] Yen, Teh Fu, J. Gordon Erdman, and Sidney S. Pollack, Investigation of the structure of petroleum asphaltenes by X-ray diffraction, *Analytical chemistry,* 1961, 33(11), 1587-1594.

[4] He, Z., Jiang, S., Li, Q., Wang, J., Zhao, Y. and Kang, M., Facile and cost-effective synthesis of isocyanate microcapsules via polyvinyl alcohol-mediated interfacial polymerization and their application in self-healing materials, *Composites Science and Technology*, 2017, *138*, 15-23.

[5] Bonakdar, S., Emami, S.H., Shokrgozar, M.A., Farhadi, A., Ahmadi, S.A.H. and Amanzadeh, A., Preparation and characterization of polyvinyl alcohol hydrogels crosslinked

by biodegradable polyurethane for tissue engineering of cartilage, *Materials science and engineering: c*, 2010, *30*(4), 636-643.

[6] Ketren, W., Zen, H., Ashida, R., Kii, T. and Ohgaki, H., Investigation on Conversion Pathways in Degradative Solvent Extraction of Rice Straw by Using Liquid Membrane-FTIR Spectroscopy, *Energies*, 2019, *12*(3), p.528.

[7] Hou, R., Bai, Z., Hao, P., Dai, X., Xu, J., Zheng, H., Guo, Z., Kong, L., Bai, J. and Li, W., Effects of temperature and solvents on structure variation of Yunnan lignite in preheating stage of direct liquefaction, *Fuel*, 2019, *239*, 917-925.

[8] Liu, X., Hirajima, T., Nonaka, M., Mursito, A.T. and Sasaki, K., Use of FTIR combined with forms of water to study the changes in hydrogen bonds during low-temperature heating of lignite, *Drying technology*, 2016, *34*(2), 185-193.

[9] Bledzki, A.K., Mamun, A.A. and Volk, J., Barley husk and coconut shell reinforced polypropylene composites: the effect of fibre physical, chemical and surface properties, *Composites Science and Technology*, 2010, *70*(5), 840-846.